IOPscience iopscience.iop.org

Home Search Collections Journals About Contact us My IOPscience

Real-space and energy representations for the interface-roughness scattering in quantum-well structures

This article has been downloaded from IOPscience. Please scroll down to see the full text article.

2001 J. Phys.: Condens. Matter 13 1259

(http://iopscience.iop.org/0953-8984/13/6/306)

View the table of contents for this issue, or go to the journal homepage for more

Download details:
IP Address: 171.66.16.226
The article was downloaded on 16/05/2010 at 08:34

Please note that terms and conditions apply.

INSTITUTE OF PHYSICS PUBLISHING JOURNAL OF PHYSICS: CONDENSED MATTER

J. Phys.: Condens. Matter **13** (2001) 1259–1264 www.iop.org/Journals/cm PII: S0953-8984(01)17553-3

Real-space and energy representations for the interface-roughness scattering in quantum-well structures

S K Lyo

Sandia National Laboratories, Albuquerque, NM 87185, USA

Received 28 September 2000

Abstract

We show that the real space representation of the interface roughness as a fluctuating potential in the coordinate space is equivalent to the usual energy-fluctuation representation for intrasublevel scattering in multi-interface quantum well structures with *generally* shaped confinement-potential profiles. The coordinate picture is, however, more general and can be used for higher-order effects and multi-sublevel scattering in tunnel-coupled multi-quantum-well structures. The result is employed to study the interface-roughness-limited mobility of tunnel-coupled double quantum wells at low temperatures.

1. Introduction

Interface roughness is present in all artificially fabricated layered structures. It causes unavoidable linewidths in optical spectroscopy [1] and also limits the low-temperature mobility in modulation-doped narrow semiconductor quantum wells (QWs), heterostructures and inversion layers [2–6]. In earlier treatments, the energy fluctuation due to the interface roughness for intrasublevel scattering is given basically by

$$\delta E(\boldsymbol{r}_\parallel) = \frac{\partial E}{\partial L}\delta L(\boldsymbol{r}_\parallel) \tag{1}$$

where E is the sublevel energy and $\delta L(\boldsymbol{r}_\parallel)$ is the fluctuation of the well width L at the in-plane position $\boldsymbol{r}_\parallel$ [2–6]. The energy $\delta E(\boldsymbol{r}_\parallel)$ is suitable only for studying intrasublevel scattering in a *single* QW, a heterostructure or an inversion layer with one or two interfaces. The fluctuation energy $\delta E(\boldsymbol{r}_\parallel)$ in equation (1) is inadequate for treating more complicated problems such as structures with multiple interfaces separated by thin barriers, higher-order scattering effects or intersublevel scattering. Recently, Mou and Hong studied the effect of the distortion of the ground sublevel wave function due to the interface roughness in an infinitely deep single QW introducing a correction term to the Hamiltonian in equation (1) linear in the gradient of $\delta L(\boldsymbol{r}_\parallel)$ [6]. A similar effect was considered earlier, in silicon inversion layers, by shifting the coordinate of the confinement function rigidly by $\delta L(\boldsymbol{r}_\parallel)$ at the interface [3, 7]. This approximation is applicable only to single-interface structures. In the present paper, we generalize equation (1) to multi-interface QW structures and study a more general form for

0953-8984/01/061259+06$30.00 © 2001 IOP Publishing Ltd Printed in the UK

the scattering potential which is shown to reduce to equation (1) for intra-sublevel scattering. The effect of the interface-roughness-induced distortion of the wave function on the mobility is included in our approach microscopically by investigating higher-order corrections to the Born approximation, employing a standard diagrammatic perturbation theory. This effect yields significant (e.g. up to 25%) correction in the range of the parameters studied. The many-body effect is not considered here [6].

2. Interface roughness potential

A natural microscopic picture for the fluctuation energy for a single QW (for simplicity) is to write

$$\delta E(\boldsymbol{r}_\parallel, z) = \pm V_\pm \delta L_\pm(\boldsymbol{r}_\parallel)\delta(z \pm \tfrac{1}{2}L) \tag{2}$$

where $\delta(z)$ is the Dirac delta function and $V_l = V_+(V_r = V_-)$ is the potential-energy *discontinuity* at the left (right) interface at $z = -L/2$ ($z = L/2$) as shown in figure 1. While the expression in equation (2) is intuitively deduced from a standard perturbation theory, its validity and equivalence to the expression in equation (1) should be examined for a general confinement-potential structure, including the often used limit of infinitely deep QWs (i.e. band offsets) with $V_\pm \to \infty$. The effect of the potential in equation (2) on the distortion of the confinement wave functions is included by going beyond the Born approximation.

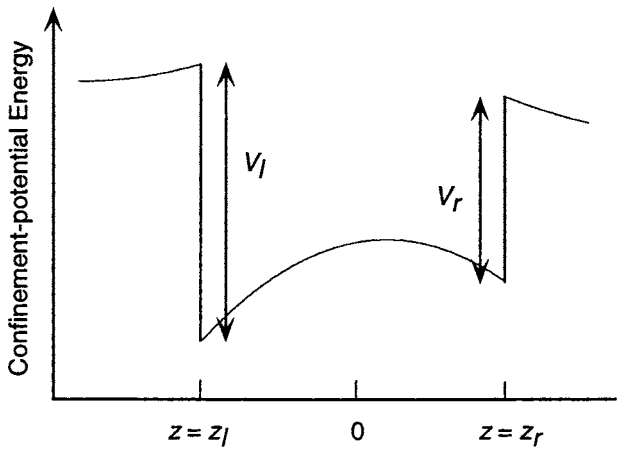

Figure 1. Confinement potential-energy for the electrons with an arbitrary band bending. The quantities V_l and V_r represent potential-energy discontinuities at the left and right interfaces at $z = z_l$ and $z = z_r$.

The inter- and intrasublevel matrix element of the potential in equation (2) is given by

$$\langle f|\delta E(\boldsymbol{r}_\parallel, z)|i\rangle = \pm V_\pm \delta L_\pm(\boldsymbol{r}_\parallel)\psi_f^*(\mp L/2)\psi_i(\mp L/2) \tag{3}$$

where $\psi_i(z)$ and $\psi_f(z)$ are sublevel functions. In order to show that equation (3) reduces to equation (1) for intrasublevel scattering for a general confinement-potential structure in a single QW, we prove the following identity:

$$\langle\psi|\delta E(\boldsymbol{r}_\parallel, z)|\psi\rangle = -V_-\delta L_-(\boldsymbol{r}_\parallel)|\psi(L/2)|^2 = \frac{\partial E}{\partial L}\delta L_-(\boldsymbol{r}_\parallel) \tag{4}$$

where $\psi(z)$ is any sublevel function with an eigenvalue E defined below in equation (5). Equation (4) is written only for the layer fluctuation at the right interface for simplicity.

For this purpose, we write the Schrödinger equation as

$$H\psi = E\psi \tag{5a}$$

$$H = H_0 + V(z) \tag{5b}$$

$$V(z) = V_l\theta(z_l - z) + V_r\theta(z - z_r) \tag{5c}$$

where H is the Hamiltonian without interface fluctuations and $V(z)$ represents the discontinuities potential-energy steps at the left ($V_l = V_+$) and right ($V_r = V_-$) interfaces at $z = z_l, z_r$ (figure 1). In equation (5*b*), H_0 is the rest of the Hamiltonian including an *arbitrary* band-bending potential profile around the interfaces in the presence of ionized dopants. We assume that there is no correlation between the interface fluctuations at the right and left interfaces at any position $\boldsymbol{r}_\parallel$ and consider only the fluctuation δz_r at the right interface for convenience. By taking a derivative with respect to z_r on both sides of equation (5*a*), using $\partial V(z)/\partial z_r = -V_r\delta(z - z_r)$, and taking an inner product from the left side with ψ^*, we find

$$\frac{\partial E}{\partial z_r} = -V_r|\psi(z_r)|^2. \tag{6}$$

This expression is identical to equation (4) if one identifies $\delta z_r = \delta L(\boldsymbol{r}_\parallel)$. Note that the effect of the wave-function distortion due to δz_r (i.e. $\partial\psi(z)/\partial z_r \neq 0$) is included in the above derivation. Note also that the above derivation of equation (6) is valid for an arbitrary interface for a generally shaped multi-QW structure.

The interesting general relationship in equation (6) can be verified for the eigenvalues and eigenfunctions of a square-well potential, for example, by tediously calculating the eigenvalues and the eigenfunctions. One can also show that the relationship holds even for an infinitely deep well. In this limit (i.e. $V_r \to \infty$), the wave function $\psi(z_r)$ in equation (6) becomes infinitesimally small (i.e. $|\psi(z_r)| \sim 1/|V_r|^{1/2} \to 0$) at the interface, cancelling the factor V_r, yielding $\partial E/\partial z_r = -\hbar^2/(m^*L^3)$ for the ground sublevel as expected.

To summarize the result so far, we have shown for generally shaped multi-QW structures that the coordinate representation of the interface-roughness scattering potential

$$\delta E(\boldsymbol{r}_\parallel, z) = -\sum_j V_j\delta L_j(\boldsymbol{r}_\parallel)\delta(z - z_j) \tag{7}$$

reduces to the generalized form of the energy fluctuation

$$\delta E_n(\boldsymbol{r}_\parallel) = \sum_j \frac{\partial E_n}{\partial z_j}\delta L_j(\boldsymbol{r}_\parallel) \tag{8}$$

for intrasublevel scattering in the nth sublevel with energy E_n. In equation (7), V_j is the algebraic potential discontinuity at the jth interface at $z = z_j$ and δL_j is the layer fluctuation.

3. Mobility in coupled double quantum wells

The result in equation (7) is now applied to study the low-temperature mobility of symmetric GaAs/Al_xGa_{1-x}As double quantum wells shown in the inset of figure 3. The QWs are $V = 250$ meV deep and 140 Å wide. The centre barrier width is 10 Å. The effective mass is $m^* = 0.67\,m_0$ in the QWs and $m^* = 0.9\,m_0$ in the barriers. The lowest two sublevels $n = 1, 2$ or $n = 1$ are occupied in the range of the electron density studied. The Boltzmann equation is given by

$$\boldsymbol{v}_{n\boldsymbol{k}} \cdot \boldsymbol{u} + \frac{2\pi}{\hbar}\sum_{n'\boldsymbol{k}'}[I_2(n'\boldsymbol{k}', n\boldsymbol{k}) + I_4(n'\boldsymbol{k}', n\boldsymbol{k})](\phi_{n'\boldsymbol{k}'} - \phi_{n\boldsymbol{k}})\delta(\varepsilon_{n'\boldsymbol{k}'} - \varepsilon_{n\boldsymbol{k}}) = 0 \tag{9}$$

where $I_2(n'\boldsymbol{k}', n\boldsymbol{k}) = \langle|\langle n'\boldsymbol{k}'|\delta E|n\boldsymbol{k}\rangle|^2\rangle_{av}$ is the Born approximation given in figure 2(a), $\boldsymbol{u}$ is a unit vector in the field direction, $\boldsymbol{v}_{n\boldsymbol{k}} = \hbar\boldsymbol{k}/m^*$ and av indicates the ensemble average. The quantity $\phi_{n\boldsymbol{k}}$ is the distribution function. The quantity $I_4(n'\boldsymbol{k}', n\boldsymbol{k})$ defined in figure 2(b) is the fourth-order correction to the Born approximation and represents scattering through the intermediate states shown by the solid lines in figure 2(b). This term reflects the effect of the wave function distortion due to the roughness. The crosses there indicate the two-site correlation relation of the layer fluctuation. The solid lines represent fermion propagators [8].

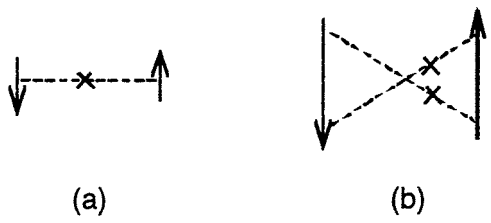

Figure 2. Irreducible scattering part including the Born approximation (a) and the fourth-order scattering through the intermediate states shown by the solid lines (b). The crosses indicate the two-site correlation of the layer function. The solid lines represent fermion propagators.

Equation (9) is solved by introducing the relaxation times τ_n at the Fermi level: $\phi_{n\boldsymbol{k}} = \tau_n \boldsymbol{v}_{n\boldsymbol{k}} \cdot \boldsymbol{u}$. We assume that the layer fluctuations at different interfaces are uncorrelated and introduce the correlation length Λ_j by $\langle\delta L_j(\boldsymbol{r}_\parallel)\delta L_{j'}(\boldsymbol{r}'_\parallel)\rangle_{av} = \delta b_j^2 \delta_{j,j'} \exp(-(\boldsymbol{r}'_\parallel - \boldsymbol{r}_\parallel)^2/\Lambda_j^2)$. The mobility equals $\mu = e\tau_{av}/m^*$ where τ_{av} is the average relaxation time $\tau_{av} = (\tau_1\varepsilon_{1F} + \tau_2\varepsilon_{2F})/(\varepsilon_{1F} + \varepsilon_{2F})$. Here $\varepsilon_{nF} \propto N_n$ is the Fermi energy and N_n is the density. The relaxation times are given by

$$\tau_1 = \frac{Q^0_{2,2} - Q^1_{2,2} + Q^0_{1,2} + Q^1_{2,1}\sqrt{\varepsilon_{2F}/\varepsilon_{1F}}}{(Q^0_{1,1} - Q^1_{1,1} + Q^0_{2,1})(Q^0_{2,2} - Q^1_{2,2} + Q^0_{1,2}) - Q^1_{2,1}Q^1_{1,2}}$$
$$\tau_2 = \tau_1 \text{ (level index } 1 \leftrightarrow 2) \tag{10}$$

where

$$Q^m_{n,n'} = \frac{2\pi^2}{\hbar A}\sum_{\boldsymbol{k}'j}(V_j\Lambda_j)^2\Psi^j_{n',n,n',n}\mathrm{e}^{-\Lambda_j^2(\boldsymbol{k}'-\boldsymbol{k})^2/4}\cos^m\theta\,\delta(\varepsilon_{n'\boldsymbol{k}'} - \varepsilon_{n\boldsymbol{k}})$$
$$+\frac{\pi^2 m^*}{2\hbar^3 A}\sum_{\boldsymbol{k}'}\sum_{j,j'}(V_jV_{j'}\Lambda_j\Lambda_{j'})^2\sum_{\nu,\nu'}\Psi^j_{n',n,\nu,\nu'}\Psi^{j'}_{\nu,\nu',n,n'}$$
$$\times\mathrm{e}^{-\Lambda^2(\boldsymbol{k}'-\boldsymbol{k})^2/8}\cos^m\theta\,\delta(\varepsilon_{n'\boldsymbol{k}'} - \varepsilon_{n\boldsymbol{k}})$$
$$\times\int_0^\infty \mathrm{d}\varepsilon\frac{\mathrm{e}^{-\varepsilon/2\varepsilon_\Lambda}}{\varepsilon_{\boldsymbol{k},\boldsymbol{k}'} + \varepsilon - (\varepsilon_{\mu\nu} + \varepsilon_{\mu\nu'})/2}\left\{\frac{\mathrm{sign}(\varepsilon_{\boldsymbol{k},\boldsymbol{k}'} + \varepsilon - \varepsilon_{\mu\nu})\theta_\nu(\varepsilon)}{\sqrt{(\varepsilon_{\boldsymbol{k},\boldsymbol{k}'} + \varepsilon - \varepsilon_{\mu\nu})^2 - 4\varepsilon_{\boldsymbol{k},\boldsymbol{k}'}\varepsilon}}\right.$$
$$\left.+(\nu \to \nu')\right\}. \tag{11}$$

Here the first term represents the contribution from $I_2(n'\boldsymbol{k}', n\boldsymbol{k})$ given in figure 2(a) and the second term is from $I_4(n'\boldsymbol{k}', n\boldsymbol{k})$ defined in figure 2(b). In equation (11), $m = 0, 1$, θ is the angle between $\boldsymbol{k}$ and $\boldsymbol{k}'$, A is the area of the QW, $\varepsilon_\Lambda = \hbar^2/2m^*\Lambda^2$ and $\varepsilon_{\boldsymbol{k},\boldsymbol{k}'} = \hbar^2 q^2/2m^*$ with $\boldsymbol{q} = (\boldsymbol{k} + \boldsymbol{k}')/2$. The quantity Ψ^j is defined by

$$\Psi^j_{n',\nu',n,\nu} = \delta b_j^2 \psi^*_{n'}(z_j)\psi^*_{\nu'}(z_j)\psi_n(z_j)\psi_\nu(z_j). \tag{12}$$

The ε-integration in the second term of equation (11) takes the principal part. The quantity $\theta_\nu(\varepsilon)$ equals unity when the argument of the square root in the denominator under it is positive

and vanishes otherwise. We further define $\varepsilon_{\mu\nu} = \mu - \varepsilon_\nu$ where μ is the chemical potential and ε_ν is the νth sublevel. The summation of the intermediate states ν converges rapidly and it was sufficient to sum up to $\nu = 8$ for the application to be presented below. The second term in equation (11) is written only for the case where $\Lambda_j \equiv \Lambda$ is independent of the interface, for simplicity. For single-level occupation, the mobility is given by $\mu = e\tau_1/m^*$: $\tau_1^{-1} = Q^0_{1,1} - Q^1_{1,1}$ in equation (10).

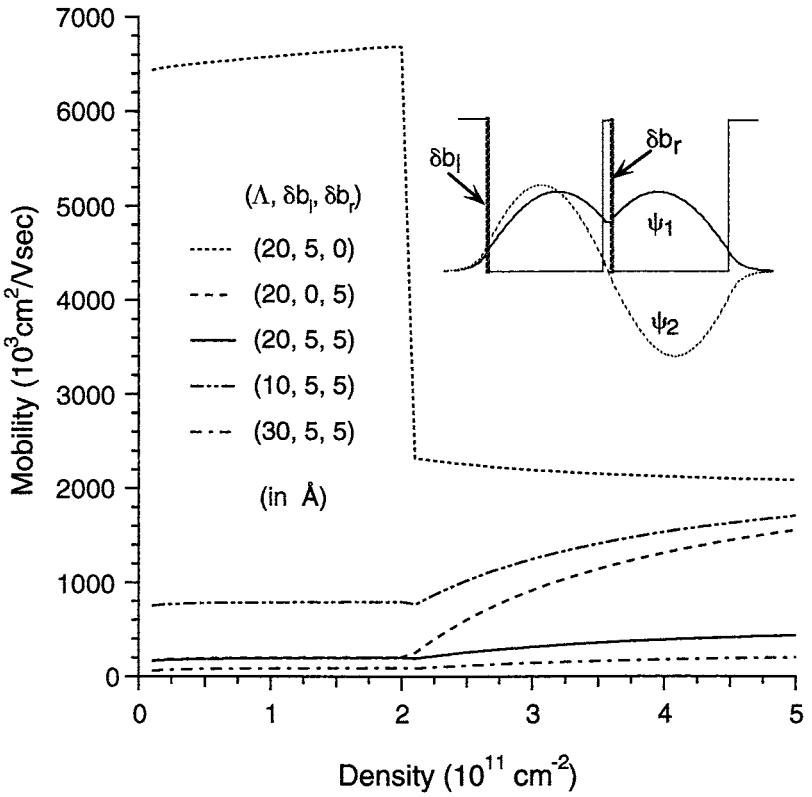

Figure 3. Electron mobility of 140–10–140 Å symmetric GaAs/$Al_xGa_{1-x}As$ double quantum wells as a function of the electron density. The interface roughness is indicated by thick hatched vertical lines in the inset, where the wave functions are plotted for the levels $n = 1, 2$. The quantities Λ, δb_l and δb_r are the correlation length and the amplitudes of the layer fluctuation in units of Å.

4. Applications and discussion

The mobility is displayed in figure 3 as a function of the electron density for $\Lambda_j = 20$ Å for three cases. Interface roughness is assumed to be significant only at the two interfaces shown by the thick hatched vertical lines in the inset of figure 3, as occurs in typical GaAs/$Al_xGa_{1-x}As$ double QWs. The solid curve represents the case where the fluctuation amplitudes are $\delta b_l = \delta b_r = 5$ Å at both interfaces. In this case, the mobility begins to rise slowly above the density $N^* = 2.1 \times 10^{11}$ cm^{-2}, when the electrons begin to populate the $n = 2$ level. The wave function $\psi_2(z)$ of these electrons has a node at the centre of the centre barrier. As a result, these electrons barely see the roughness δb_r, raising the net mobility. This enhancement effect is subdued somewhat, however, due to the fact that $\psi_2(z)$ has more penetration into the

δb_1 interface than $\psi_1(z)$. The mobility is low for the solid curve as a whole mainly because $\psi_1(z)$ has a large amplitude at the δb_r interface as seen in the inset of figure 3. This fact makes the mobility low (compared to the dotted curve in figure 3) even for the case $\delta b_1 = 0$, $\delta b_r = 5$ Å (dashed curve) below N^*, although it is slightly higher than that of the solid curve because $\delta b_1 = 0$. Above N^*, however, the dashed curve rises much faster than the solid curve, because the enhanced amplitude of $\psi_2(z)$ at the $\delta b_1 (= 0)$ interface does not affect the mobility. For $\delta b_1 = 5$, $\delta b_r = 0$ Å (dotted curve), the mobility is very high below N^* because the wave function $\psi_1(z)$ has a small amplitude at the δb_1 interface. Above N^*, however, the wave function $\psi_2(z)$ has a much larger amplitude than $\psi_1(z)$ at the δb_1 interface, lowering the mobility nearly by a factor of three.

In the above analysis, the Fermi wave numbers are small, k_{1F}, $k_{2F} < 0.0178$ Å^{-1}, for $N < 5 \times 10^{11}$ cm^{-2} studied in figure 3, yielding $k_{nF}\Lambda_j < 1$ for $\Lambda_j = 20$ Å employed. As a result, the density dependence of the factor $\exp[-\Lambda_j^2(\boldsymbol{k}' - \boldsymbol{k})^2]$ in equation (11) is weak. For a long correlation length Λ_j such that $k_{nF}\Lambda_j > 1$, however, the rate constant $Q^m_{n,n'}$ in equation (11) can have a strong dependence on the density through this factor. In this case, the mobility rises more rapidly with N in each section (i.e. $N < N^*$ and $N > N^*$) of the horizontal axis in figure 3.

The mobility depends on the correlation length as shown by the dash–dotted ($\Lambda = 30$ Å) and dash–double-dotted ($\Lambda = 10$ Å) curves in figure 3. The fourth-order correction reduces the mobility significantly in the low-mobility regime. For example, the reduction is about 25% for the dash–dotted curve in the low-density region $N < 10^{11}$ cm^{-2} in figure 3 but is much smaller elsewhere.

We have also studied the mobility of a *single* QW as a function of the density for occupations up to the second sublevel. The density-dependent behaviour is very similar to the $\delta b_1 = 5$, $\delta b_r = 0$ Å case shown by the dotted curve in figure 3, as is expected.

5. Summary

In summary, we have shown that the coordinate representation of the interface-roughness scattering potential in equation (7) reduces to the generalized form of the usual energy-fluctuation model in equation (8) for intrasublevel scattering. The representation in equation (7) is useful in treating multi-sublevel scattering in coupled multi-QWs [9]. The result was employed to study the interface-roughness-limited mobility of coupled double QWs.

Acknowledgments

Sandia is a multiprogram laboratory operated by Sandia Corporation, a Lockheed Martin Company, for the US DOE under contract No DE-AC04-94AL85000.

References

[1] Tanaka M, Sakaki H and Yoshino J 1986 *Japan. J. Appl. Phys.* **25** L155
[2] Sakaki H, Noda T, Hirakawa K, Tanaka M and Matsusue T 1987 *Appl. Phys. Lett.* **51** 1934
[3] Ando T 1977 *J. Phys. Soc. Japan* **43** 1616
[4] Laijhtman B and Kiehl R A 1993 *Phys. Rev.* B **47** 10 515
[5] Gold A 1987 *Phys. Rev.* B **35** 723
[6] Mou C Y and Hong T 2000 *Phys. Rev.* B **61** 12 612
[7] Ando T, Fowler A B and Stern F 1982 *Rev. Mod. Phys.* **54** 437
[8] Fetter A L and Walecka J D 1971 *Quantum Theory of Many-Particle Systems* (New York: McGraw-Hill)
[9] Huang D and Lyo S K 2000 *J. Phys.: Condens. Matter* **12** 3383